

24.4% industrial tunnel oxide passivated contact solar cells with ozone-gas oxidation Nano SiO_x and tube PECVD prepared in-situ doped polysilicon

Zunke Liu ^{a,b,c,1}, Na Lin ^{f,a,c,1}, Qingshan Zhang ^d, Bin Yang ^e, Lihua Xie ^d, Yan Chen ^e, Wangpeng Li ^d, Mingdun Liao ^{a,c}, Hui Chen ^d, Wei Liu ^{a,c}, Yuming Wang ^d, Shihua Huang ^f, Baojie Yan ^{a,b,c}, Yuheng Zeng ^{a,b,c,d,*}, Yimao Wan ^{e,**}, Jichun Ye ^{a,b,c,***}

^a Ningbo Institute of Materials Technology and Engineering, Chinese Academy of Sciences, Ningbo City, Zhejiang Province, 315201, PR China

^b University of Chinese Academy of Sciences, Beijing, 100049, PR China

^c Zhejiang Engineering Research Center for Energy Optoelectronic Materials and Devices, Ningbo Institute of Materials Technology & Engineering, CAS, Ningbo City, Zhejiang Province, 315201, PR China

^d Suzhou Tuosheng Intelligent Equipment Co., Ltd (subsidiary Company of Yingkou Jinchen Machinery Co., Ltd), Suzhou City, Jiangsu Province, 215156, PR China

^e Risen Energy Co., Ltd, Ningbo City, Zhejiang Province, 315609, PR China

^f Provincial Key Laboratory of Solid State Optoelectronic Devices, Zhejiang Normal University, Jinhua City, Zhejiang Province, 321004, PR China



ARTICLE INFO

Keywords:

Ozone gas oxidation (OGO)

Tunnel oxide

Tube PECVD

TOPCon

ABSTRACT

Ozone-gas oxidation (OGO) technology, capable of integrating into tube plasma-enhanced chemical vapor deposition (PECVD) technology, is developed to prepare the Nano SiO_x layer for tunnel oxide passivated contact (TOPCon) solar cells in this work. The effects of gas flow, oxidation temperature, and annealing temperature on passivation quality are investigated. The X-ray photoelectron spectroscopy (XPS) indicates that OGO SiO_x possesses a Si⁴⁺ proportion of about 20%, higher than the nitric acid oxidized (NAOS) SiO_x and plasma-assisted N₂O oxidation (PANO) SiO_x. The implied open-circuit voltage (*iV_{oc}*) of the hydrogenated lifetime sample is promoted to more than 740 mV with the highest value of 748 mV, corresponding to a lowest single-sided saturation current density (*J_{0,s}*) of 3.1 fA/cm². The contact resistivity extracted from the Cox-Strack method is < 9 mΩ cm² as the annealing temperature is more than 840 °C. Finally, we prepared the large-sized TOPCon solar cells with an average efficiency of 24.37% and a maximum efficiency of 24.41%, respectively. The above work shows that the tube PECVD technology integrated with ozone gas oxidation has the potential for the mass-production TOPCon industry.

1. Introduction

Tunnel oxide passivated contact (TOPCon), featuring a Nano silicon oxide (SiO_x) layer and a heavily doped polycrystalline silicon (polysilicon) film inserted between the silicon wafer and metal electrodes, is considered as one of the most promising passivating contact technologies [1–4]. This structure simultaneously achieves excellent surface passivation and carrier selective collection [5] and has enabled the efficiency of the industrial n-type silicon solar cells over 24.5% [6].

Meanwhile, TOPCon technology has the advantages of compatibility with the existing passivated emitter and rear contact (PERC) production lines [7,8], i.e., the PERC line can be upgraded to the high-efficiency TOPCon line by adding several key equipment for preparing the boron emitter, Nano SiO_x, and heavily-doped polysilicon. TOPCon has been widely regarded as the next-generation dominant high-efficiency crystalline silicon solar-cell technology after PERC [9].

Developing proper tools to fabricate the high-quality Nano SiO_x and heavily-doped polysilicon is one of the most critical factors to promote

* Corresponding author. Ningbo Institute of Materials Technology and Engineering, Chinese Academy of Sciences, Ningbo City, Zhejiang Province, 315201, PR China., .

** Corresponding author., .

*** Corresponding author. Ningbo Institute of Materials Technology and Engineering, Chinese Academy of Sciences, Ningbo City, Zhejiang Province, 315201, PR China., .

E-mail addresses: yuhengzeng@nimte.ac.cn (Y. Zeng), wanyi@risenenergy.com (Y. Wan), jichun.ye@nimte.ac.cn (J. Ye).

¹ Zunke Liu and Na Lin contributed equally to this work.

the industrial application of TOPCon solar cells [10]. Tube plasma-enhanced chemical vapor deposition (PECVD) is considered as a promising technology for mass production of TOPCon cells in comparison with the dominant low-pressure chemical vapor deposition (LPCVD) tool since this technology exhibits the advantages of the higher film deposition rate, the deposition of in-situ doped amorphous silicon (a-Si:H), the slighter wrap-round deposition, and the avoidance of a-Si:H deposition on the quartz tube [11,12]. The tube PECVD route shows the potential to simplify the fabrication processes of TOPCon cells and save cost. Fraunhofer ISE has already demonstrated that tube PECVD technology can prepare the high-performance in-situ doped a-Si thin films, which enables to obtain excellent passivation quality with an implied V_{oc} (iV_{oc}) of above 735 mV and an efficiency of ~23% (M2-sized with metallization achieved by screen-printing) [11,12].

However, one of the issues blocking the application of the tube PECVD technology is the lack of a successfully proven high-quality in-situ oxidation technology compatible with graphite-boat carriers. The graphitic boat as the standard carrier of tube PECVD cannot withstand the current industry-used thermal oxidation process, typically more than 600 °C, making it impossible to use thermal oxidation technology directly. On the other hand, if the Nano SiO_x is fabricated by thermal oxidation, it will require to transfer the wafers from quartz boat to graphite boat by automated equipment. However, it would raise another concern that the robotic arms and the exposure to the environment may be harmful to the interfacial SiO_x . Based on the above analysis, developing an in-situ oxidation technology compatible with graphite boats is of great significance in promoting tube PECVD to mass production.

Ozone oxidation is a well-proven method to prepare high-quality Nano SiO_x at low temperatures [13] and shows the potential of compatibility with graphite boats. Fraunhofer ISE has previously investigated the ultraviolet photo-oxidation (UV/ O_3) and ozone-water oxidation (DIO₃) for TOPCon-used Nano SiO_x [14,15], obtaining excellent passivation quality with the implied open-circuit voltage (iV_{oc}) of >720 mV on planar wafers, which demonstrate the feasibility of ozone oxidation. However, both the UV/ O_3 and DIO₃ methods could not be compatible with industrial applications. Plasma-assisted oxidation is another technology able to integrate with tube PECVD technology [16]; however, it unavoidably introduces ion-bombardment-induced defects [17] that degrade passivation quality more or less.

In this work, we have developed an ozone gas (O_3) oxidation technique compatible with the industrial tube PECVD technology and enables us to simultaneously prepare the Nano SiO_x layer and in-situ doped a-Si with one set of graphite boat carrier. The double-sided passivated lifetime wafers based on n-type planar silicon substrates manifest an initial iV_{oc} of over 735 mV after high-temperature annealing and more than 745 mV after hydrogenation with AlO_x . The champion iV_{oc} reaches 748 mV, with the corresponding single-sided saturated current density ($J_{0,s}$) of 3.1 fA/cm². Meanwhile, the average efficiency of industrial large-sized n-type TOPCon solar cells reaches 24.37%. This contribution has proven the practicability of the tube PECVD technology route with ozone-gas oxidation for the industrial high-efficiency TOPCon solar cells.

2. Experimental details

The <100>-oriented, 158.75 mm × 158.75 mm (G1-sized), n-type Czochralski wafers with a resistivity of 0.5–1 Ωcm were used as the substrates for lifetime samples and solar cells. The descriptions of fabrication processes of the lifetime samples are as follows. The front and rear surface damage layers were removed by texturing etching, and then the textures were removed by $\text{HNO}_3\text{-HF-H}_2\text{O}$ acid etching. After removing the native SiO_x , the wafers were inserted vertically onto the graphite boat and pushed into a quartz tube for ozone gas oxidation. The interface Nano SiO_x layer was fabricated by high-concentration ozone gas oxidation process. The oxidation processes were carried out in the temperature range of 200 °C–300 °C, with the ozone flow ranging from 5

SLM to 12 SLM. The oxidation time was set as 5 min to ensure sufficient oxidation and the growth of SiO_x into the saturation stage that the growth rate becomes slow. After oxidation, an in-situ phosphorus-doped a-Si film with a thickness of 120 nm is deposited by a direct plasma source with a frequency of 40 kHz and SiH_4 , PH_3 , and H_2 as the gas precursors. Subsequently, the annealing at 800 °C–900 °C for 30 min is carried out to crystallize polycrystalline silicon and activate phosphorus impurity. Finally, the AlO_x was deposited by plate-PECVD technique with a substrate temperature of 320 °C, followed by annealing at 450 °C for 30 min to achieve hydrogenation.

The instructions of fabrication processes of the TOPCon solar cell are as follows. The wafers were textured by the KOH alkaline solution etched. The front boron-doped emitter was formed by high-temperature BCl_3 diffusion, and the rear wrap-round boron diffusion surface was polished by $\text{HNO}_3\text{-HF-H}_2\text{O}$ acid. The SiO_x was formed by ozone gas oxidation at 260 °C, and in-situ phosphorus-doped a-Si: H was deposited by the tube PECVD. The 840 °C high-temperature annealing was carried out in the quartz tube furnace. After removing the edge wrap-round deposition of polysilicon with hot KOH solution, the front and rear sides were capped by the plate-PECVD deposited AlO_x and tube-PECVD deposited SiN_x stack layers. Finally, the nine-busbar electrode pattern is fabricated by screen printing Ag-Al paste on the front and Ag paste on the rear, followed by belt-furnace firing.

We used the JC-432-1D/TS R&D tube PECVD equipment produced by Suzhou TuoSheng Intelligent Equipment Co., Ltd. The tube PECVD is equipped with a quartz tube featuring an inner diameter of 528 mm and a length of 3300 mm. The graphite boat can load 416 pieces of 158.75 mm wafers at once. We used the free-demo R&D ozone equipment to produce high-concentration O_3 gas with the maximum value of 300 g/(m³ hrs).

The effective lifetime is characterized using a Sinton (WCT-120) system, whose transient mode was used to extract the implied open-circuit voltage (iV_{oc}) and single-sided saturated current density ($J_{0,s}$). The Nano SiO_x layer was characterized using X-ray photoelectron spectroscopy (XPS) (AXIS ULTRA DLD), the transmission electron microscopy (TEM) (ThermoFisher, Talos F200×), and the energy dispersive spectrometer (EDS). The active phosphorus profile was measured using an electrochemical capacitance-voltage (ECV) system (Buchanan, CVP21). The contact resistivity was extracted from Cox-Strack (CS) method by depositing circular-dot Ag electrodes on the surface of polysilicon using thermal evaporation technique. The solar cell performance is characterized using an industrial solar simulator.

3. Results and discussion

The effects of ozone gas flow, oxidation temperature, and annealing temperature on surface passivation are investigated because these parameters determine the oxidation conditions and the SiO_x 's quality. All the oxidation processes lasted 5 min to ensure complete oxidation. Fig. 1 (a) shows the effects of the ozone gas flow on passivation quality, for which the oxidation temperature is set as 200 °C and the high-temperature annealing set as 820 °C. The observations are listed as follows. 1) The passivation quality is improved gradually as the growth of ozone gas flow, i.e., an average iV_{oc} is only 657 mV with the 5 SLM flow, while it grows to ~700 mV with the 8–10 SLM flow. 2) However, as the ozone-gas flow further increases, the passivation quality will decay. It is speculated that, on the one hand, a low gas flow may lead to a shortage of ozone gas supply and insufficient oxidation. On the other hand, the passivation is reduced as the ozone-gas flow reaches 12 SLM. It is speculated that the vast gas flow dilutes the ozone concentration if the production rate of ozone gas is constant. Setting ozone gas flow as 8 SLM is acceptable in this experiment.

Fig. 1(b) shows the effects of oxidation temperature ranging from 200 °C to 300 °C on passivation, for which the ozone-gas flow is set as 8 SLM and the high-temperature annealing as 840 °C. We can observe that the oxidation temperature influences the optimal annealing temperature

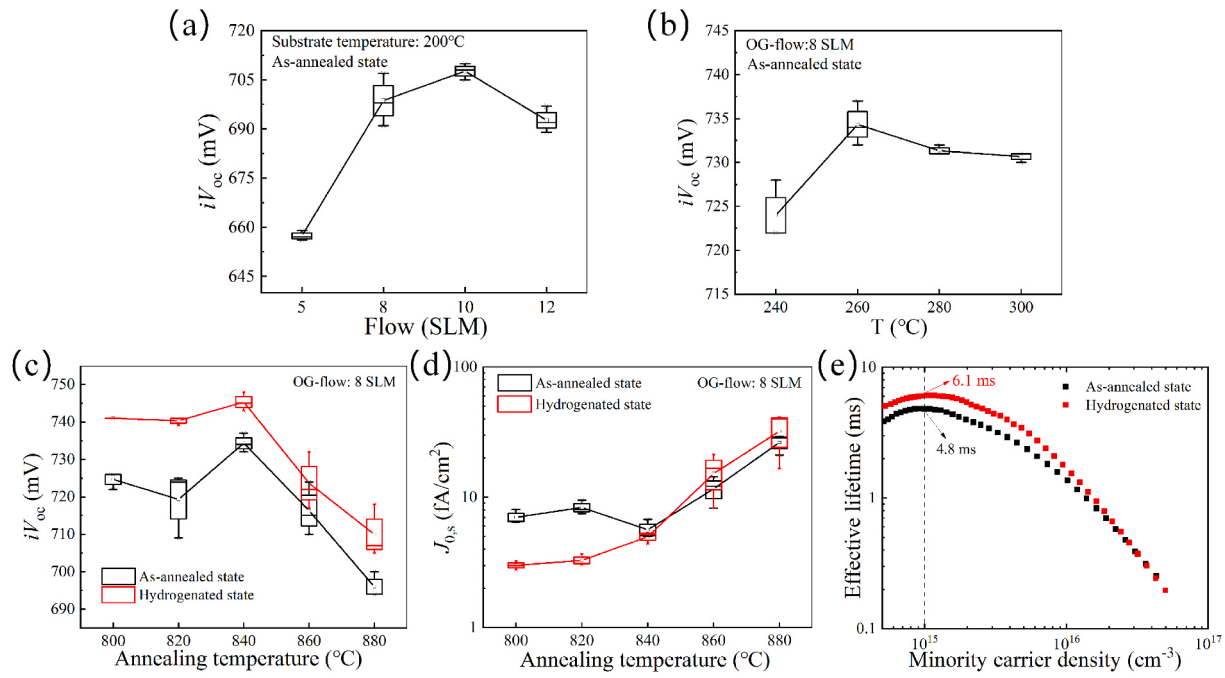


Fig. 1. (a) Effects of ozone gas flow, (b) ozone oxidation temperature, and (c), (d) annealing temperature on passivation quality, including iV_{oc} and $J_{0,s}$. (e) Effective carrier lifetime versus the excess carrier density of the champion lifetime sample without or with AlO_x hydrogenation. It should be mentioned that the as-annealed lifetime sample is capped by $\text{SiO}_x/\text{polysilicon}$, while the hydrogenated lifetime sample is capped by $\text{SiO}_x/\text{polysilicon}/\text{AlO}_x$.

and the passivation quality. The oxidation temperature also has a significant effect on the optimum passivation quality. As the oxidation temperature gradually increases, the optimal passivation quality also gradually increases. The average iV_{oc} of the as-annealed samples is 698 mV with the 200 °C oxidation temperature (shown in Fig. 1(a)), while it becomes over 735 mV with the 260 °C oxidation temperature. However, when the oxidation temperature gradually increases to more than 260 °C, the optimal passivation quality does not improve significantly, and the iV_{oc} gradually approaches stability.

Fig. 1(c and d) show the effects of the annealing temperature on the passivation quality, including iV_{oc} and $J_{0,s}$, for which the ozone-gas flow is set as 8 SLM and the oxidation temperature as 260 °C. We can observe the following phenomena. 1) For the as-annealed lifetime sample, the passivation quality is first improved with the annealing temperature ranging from 800 °C to 840 °C; and the best iV_{oc} reaches 735 mV by 840 °C annealing. 2) However, the passivation quality decays if the annealing temperature is ≥ 860 °C, which typically results from the disruption of the integrity of the interfacial SiO_x by high temperature [18] and the aggravation of Auger recombination due to excessive diffusion of P (shown in Fig. 3. (b)). 3) The passivation quality is promoted significantly after hydrogenation by AlO_x . The lifetime sample with 260 °C-grown OGO SiO_x and 840 °C annealing achieves the maximum iV_{oc} of 748 mV and the corresponding minimum $J_{0,s}$ of 3.1 fA/cm². 4) The lifetime spectrum of the champion lifetime sample is given in Fig. 1(e). The lifetimes of the as-annealed and hydrogenated samples are 4.8 ms and 6.1 ms at $1 \times 10^{15} \text{ cm}^{-3}$ minority carrier density, respectively.

Fig. 2 show the SEM image for (a) top view, (b) cross-section view, and (c) the enlarged cross-section view of the acid-etched surface capped by the OGO SiO_x and polysilicon annealed at 840 °C. It is observed that the surface is free of blistering, which is the precondition to achieve excellent passivation quality [19]. Moreover, it is found that the edges and bottoms of the irregular-sized etched pits are covered by the polysilicon film well. The excellent uniform of tube PECVD deposited silicon film for the acid-etched surface is helping to achieve excellent passivation quality.

Fig. 2(d) and (e) show the TEM image, high-resolution TEM image of

the OGO SiO_x (260 °C) and the as-deposited amorphous silicon (a-Si: H), respectively. The SiO_x layer inserted between the crystalline silicon (c-Si) substrate and the a-Si: H film shows uniform thickness across the interface, indicating that the ozone-gas oxidation method can produce micro uniformity of interfacial SiO_x . Moreover, the interface between the OGO SiO_x and the c-Si is clear compared to the unclear interface of PANO SiO_x reported by our previous work [16,20], which is an indicator of the excellent material quality. The high-resolution TEM image indicates that the OGO SiO_x is about 1.4 ± 0.2 nm, thinner than the typical thickness of the TO SiO_x (~1.8–2.0 nm) [21]. Due to the reduced thickness of the OGO SiO_x layer, its optimal annealing temperature should be lower than the commonly used temperature for TO SiO_x , ~900 °C ± 20 °C, which agrees with our observation that the optimal annealing temperature for OGO SiO_x ranges from 840 °C to 860 °C. In addition, it is observed a dark contract band with a width of ~1.5–2 nm and a shallower contract band with a width of ~10 nm under the interfacial SiO_x . The presence of contrast indicates that the preparation of SiO_x and a-Si: H may introduce lattice stress.

As shown in Fig. 2(f and g), the EDS spectra show that the distribution of interfacial oxygen elements is not limited to ~1.4 nm but shows a range of several nanometers, suggesting that oxygen atoms may diffuse during a-Si: H deposition and annealing. This observation suggests that the interfacial SiO_x is an entity with a transition zone with a gradual component.

Fig. 2(h and i) shows the XPS spectrum of SiO_x prepared by the 260 °C ozone oxidation. Meanwhile, the XPS spectra of the controlled SiO_x prepared by nitric acid oxidation SiO_x (NAOS), plasma-assisted N_2O oxidation (PANO) SiO_x , and thermal oxidation (TO) SiO_x reported by our previous works [21] are also exhibited for a comprehensive comparison. All the XPS spectra are normalized for easy comparison. The peak of Si 2p bonding-energy is used to analyze the stoichiometry of the SiO_x , i.e., the peaks of Si 2p_{3/2} and Si 2p_{1/2} located at 98.9 eV and 99.48 eV, respectively; while the peak of SiO_2 (Si^{4+}) locates at 103 eV. As can be seen, the OGO SiO_x shows a lower area proportion of Si^{4+} peak than the TO SiO_x , but a higher area proportion than the NAOS SiO_x and the PANO SiO_x (oxidation at 150 °C). As listed in Table 1, a deconvolution analysis reveals that the percentages of Si^{4+} are ~19.5% in OGO

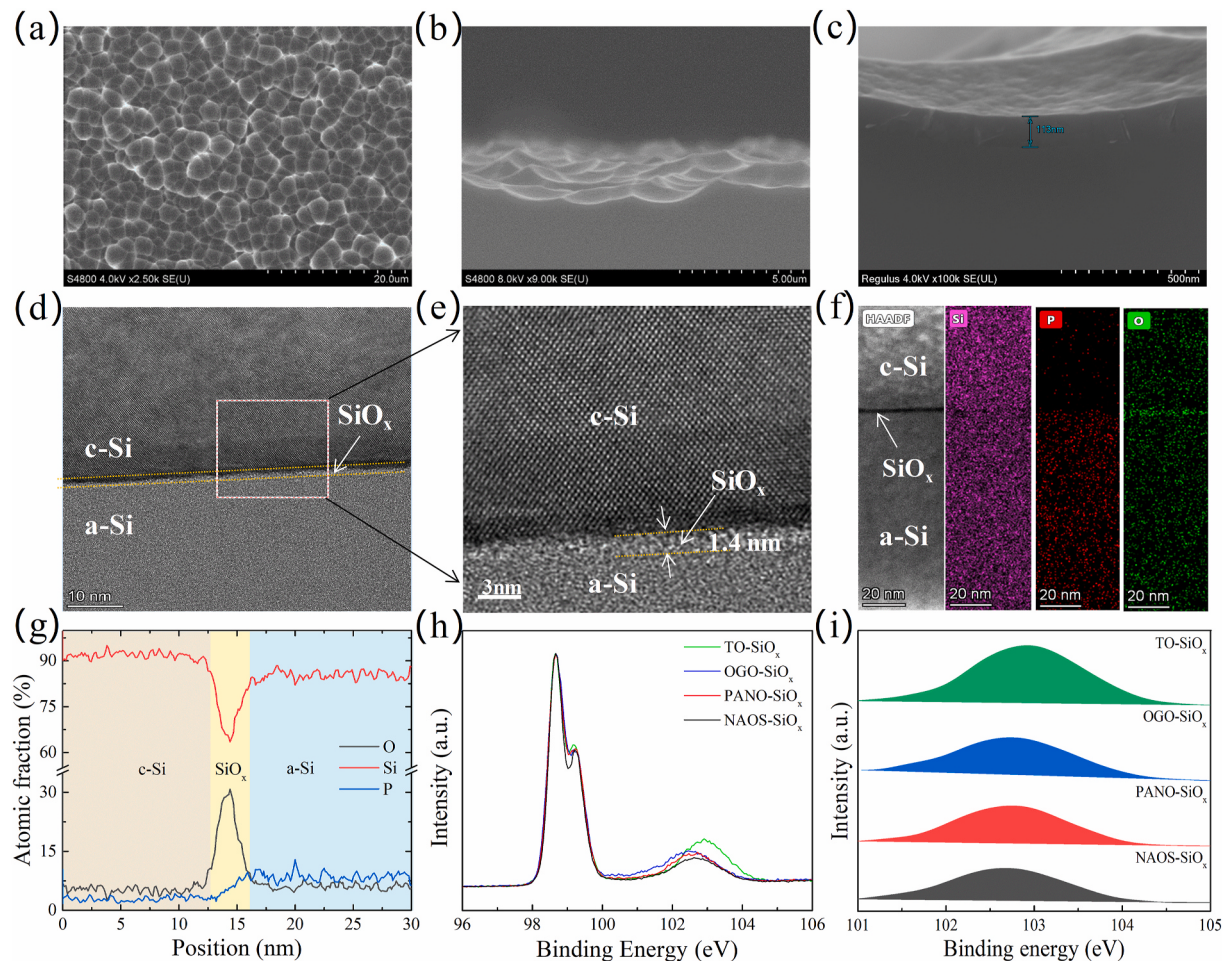


Fig. 2. (a) SEM image for top view, (b) cross-section view, and (c) the enlarged cross-section view of the acid-etched rear surface capped by the OGO SiO_x and the 840 °C annealed polysilicon. (d) TEM image and (e) high-resolution TEM image, and (f), (g) element distribution of the interfacial structure capped by the as-grown OGO SiO_x and as-deposited phosphorus-doped a-Si:H film. (h) (i) XPS spectra of the OGO, NAOS, PANO, and TO SiO_x.

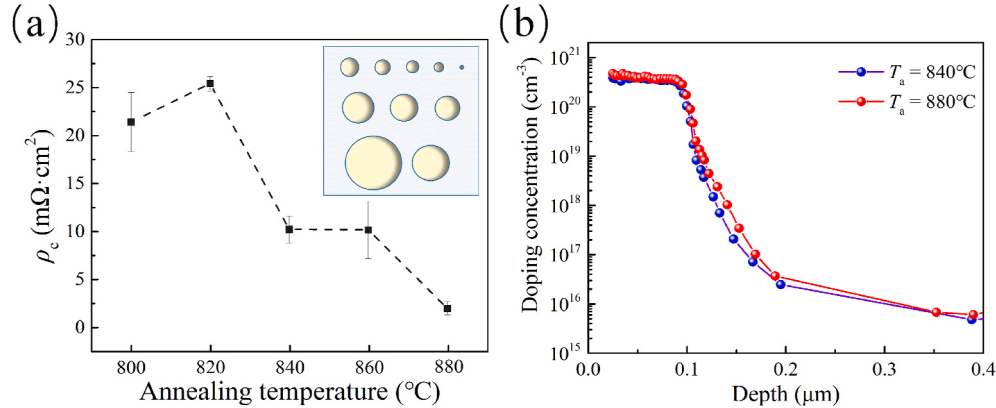


Fig. 3. (a) Effect of annealing temperature on contact resistivity, whose SiO_x is prepared by 240 °C ozone-gas oxidation. The insert is the pattern for CS measurement, with the diameters of 0.3, 0.6, 0.8, 1.0, 1.2, 1.6, 1.8, 2.0, 2.4, and 3.6 mm, respectively. (b) Activated phosphorus profile of the 840 °C and 880 °C annealed polysilicon whose SiO_x is grown by 260 °C ozone-gas oxidation.

SiO_x, ~22.5% in TO SiO_x [21], ~15%–17% in NAOS SiO_x [21,22], and ~16%–17% in PANO SiO_x [16,21]. Moreover, it is noted that the OGO SiO_x also shows a higher Si⁴⁺ proportion than that of the SiO_x oxidized by UV/O₃ with Si⁴⁺ proportion of ~13%–19%, reported by Fraunhofer ISE previously [14]. It is known that the higher percentage of the Si⁴⁺, the higher probability of obtaining excellent passivation quality. The

above observation demonstrates that the oxidation capability of ozone gas at 260 °C is acceptable, as its SiO_x shows a competitive Si⁴⁺ concentration compared to other methods. Moreover, it is worth pointing out that ozone gas oxidation free of ion bombardment compared with plasma-assisted oxidation should lead to reduced interfacial defect states.

Table 1
Statistics of Si⁴⁺ ratio in different oxidation methods.

Method	Si ⁴⁺ ratio (%)
OGO (this work)	~19.5
UV/O ₃	~13-19
NAOS	~15-17
PANO	~16-17
TO	~22.5

It is well known that TOPCon structure requires the preparation of high-quality SiO_x with sufficient oxidation and proper thickness for achieving passivation and carrier collection simultaneously [23]. The above results indicate that the preparation of ultra-thin SiO_x by ozone gas has four advantages. 1) Ozone gas oxidation will produce high-quality SiO_x. That the oxidation capability of ozone gas is strong and leads to sufficient high-valence oxidized Si, beneficial to promote passivation quality. 2) Ozone gas oxidation is suitable for achieving a low interfacial state. Actually, ozone oxidation has been widely used in the semiconductor industry. The SiO_x interface is very clear, indicating a low concentration of interfacial state, just as shown by the TEM image. Moreover, ozone oxidation, different from plasma-assist oxidation, is free of ion bombard and benefits for reducing interfacial state. 3) The oxidation temperature is lower than 300 °C. As the temperature increases, the oxidizing property of ozone also increases; therefore, increasing the temperature is beneficial to enhance the oxidation degree. However, on the other hand, the ozone's lifetime decreases significantly as the temperature increases [24–26], leading to weakened oxidation capability. Thus, choosing the appropriate annealing temperature is a trade-off for this oxidation technology. From this experimental work, the optimized ozone oxidation temperature is below 300 °C, which is suitable for saving the electric cost and extending the lifetime of graphite boats. Moreover, the corresponding optimal high-temperature annealing is only 840 °C, which is an advantage to save the production cost. 4) The thickness of silicon oxide is easy to control. Another advantage of ozone oxidation is that the growth of SiO_x is self-saturation [27], i.e., the SiO_x thickness tends to an up-limited value with the increase of time. In addition, the growth rate of silicon

oxide is low at <300 °C, which helps to offset the effects of temperature fluctuation and process-time fluctuation on SiO_x thickness. Thus, low-temperature ozone gas oxidation is favorite to prepare uniform Nano SiO_x with effortless control.

Contact resistivity (ρ_c) is another critical parameter for preparing a high-efficiency solar cell; herein, we used the CS method to test the contact resistivity of the TOPCon structure, including the interface of c-Si/SiO_x/poly-Si and interface of poly-Si/metal. Since a thick polysilicon film for CS measurement results in inaccurate contact resistivity [28], the polysilicon film is etched by immersing into HNO₃ and HF alternately and achieves a final thickness of 20–30 nm. The circular-dot metal Ag electrode pattern is deposited by the thermal evaporation technique. It is found that the ρ_c gradually decreases with increasing annealing temperature, as shown in Fig. 3(a). The ρ_c is 21.3 mΩcm² when the annealing temperature is 800 °C, while the ρ_c is lower than 9 mΩ cm² when the annealing temperature rises to 840 °C, which has been satisfied for preparing a high-efficiency solar cell. Moreover, the corresponding activated phosphorus profile produced by 840 °C annealing is determined by ECV, as given in Fig. 3(b). The activated phosphorus concentration in polysilicon is $3\text{--}4 \times 10^{20}$ cm⁻³, and the activated phosphorus concentration is reduced to 1×10^{18} cm⁻³ at a depth of 140 nm. EDNA 2 calculation indicates that the Auger-limited saturation current density originated from the in-diffusion of active phosphorus is only ~ 0.3 fA/cm², suggesting the primary recombination is likely from the interfacial defects.

Fig. 4(a) shows the schematic structure of the mass-production high-efficiency n-type TOPCon solar cell (158.75×158.75 mm²), which adopts the 260 °C-grown OGO SiO_x and the subsequent 840 °C high-temperature annealing for preparing the rear TOPCon structure. The front and rear electrodes are fabricated through screen printing and belt-furnace firing. The distribution of the critical parameters of one batch cells, including the efficiency (η), open-circuit voltage (V_{oc}), short-circuit current (I_{sc}), and fill factor (FF), are given in Fig. 4(b). It is found that the distributions of V_{oc} , I_{sc} , FF, and η are 711–713 mV, 10.34–10.36 A, 83.34–83.43%, and 24.35–24.41%, which manifests an average efficiency reached 24.37% with a standard deviation (STD) of <1.5%. The champion cell displays an efficiency of 24.41%, with the

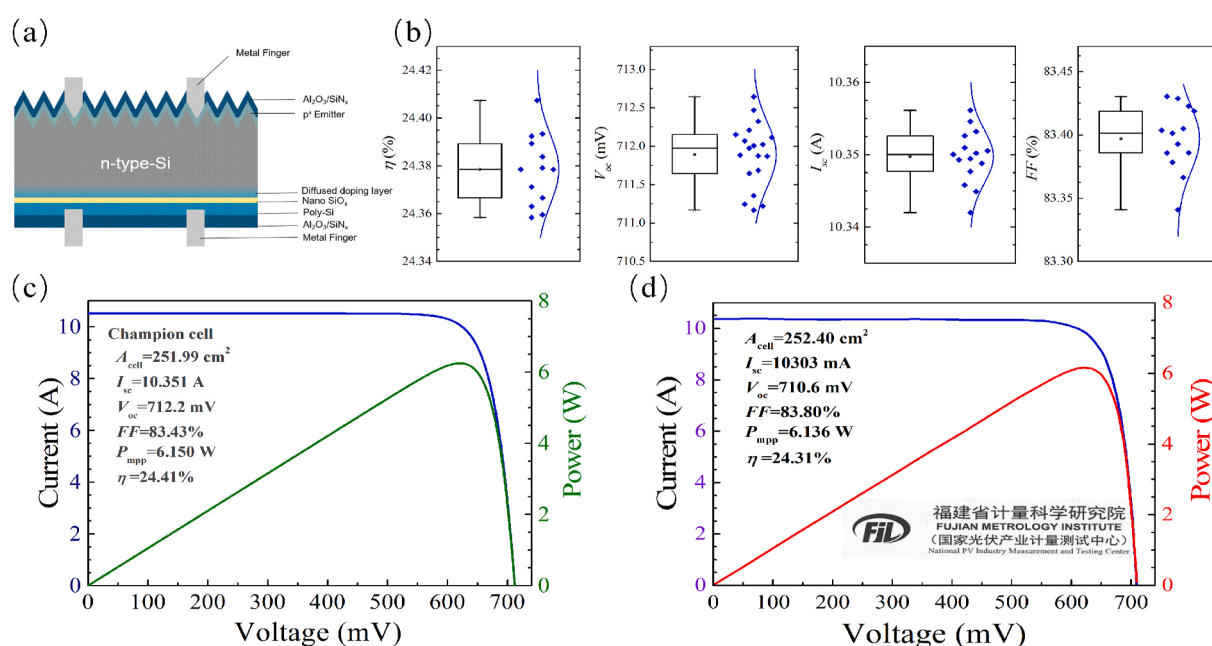


Fig. 4. (a) Schematic structure of the mass-production n-type TOPCon solar cell. (b) Statistic data of the η , V_{oc} , I_{sc} , and FF of one batch cells. (c) Voltage-current curve and voltage-power curve of the champion cell. (d) The certified voltage-current curve and voltage-power curve of the cell measured independently by National PV Industry Measurement and Testing Center. The solar cells employ the 260 °C, 8 slm grown OGO SiO_x and the subsequent 840 °C high-temperature annealing to prepare the rear TOPCon structure.

corresponding V_{oc} of 712.2 mV, I_{sc} of 10.35 mA/cm², and FF of 83.43%, as shown in Fig. 4(c). Moreover, the certified efficiency, 24.31%, measured independently by National PV Industry Measurement and Testing Center, is also given in Fig. 4(d). In comparison, the current top-level mass-production TOPCon solar cells reported by Jinko and LONGi show the efficiency of ~24.5% [6], which is produced using low-pressure chemical vapor deposition (LPCVD) technology route. Therefore, the result demonstrates that the tube PECVD technology route integrated with ozone-gas oxidation has exhibited the potential for application of industrial mass-production.

4. Summary

We have investigated the ozone-gas oxidation technology for preparing the Nano SiO_x layer and its integration in tube PECVD for industrial high-efficiency TOPCon solar cells. The preparation conditions of developing the high-quality OGO SiO_x have been studied. The ozone-gas oxidation process is lower than 300 °C, compatible with the existing tube PECVD technology. The OGO SiO_x shows a proper thickness of 1.4 ± 0.2 nm and acceptable material quality with a Si⁴⁺ proportion of ~19.5%, which is competitive with the previously reported NAOS SiO_x or PANOS SiO_x. The hydrogenated passivation lifetime samples manifest the best iV_{oc} of 748 mV and $J_{0,s}$ of 3.1 fA/cm², which has satisfied the requirement of fabricating a high-efficiency solar cell. Also, another advantage of OGO SiO_x is that the optimized high-temperature annealing is only ~840 °C, which benefits to saving the production cost. Finally, we have developed the 158.75 mm TOPCon cells with an average efficiency of 24.37% and a maximum efficiency of 24.41%. This contribution demonstrates that the tube PECVD technology integrated with ozone gas oxidation has a promising future for the mass-production TOPCon industry.

CRediT authorship contribution statement

Zunke Liu: Writing – original draft, Investigation. **Na Lin:** Investigation. **Qingshan Zhang:** Resources. **Bin Yang:** Resources. **Lihua Xie:** Resources. **Yan Chen:** Resources. **Wangpeng Li:** Resources. **Mingdun Liao:** Resources. **Hui Chen:** Resources. **Wei Liu:** Resources. **Yuming Wang:** Resources. **Shihua Huang:** Resources. **Baojie Yan:** Writing – review & editing, Conceptualization. **Yuheng Zeng:** Writing – review & editing, Conceptualization. **Yimao Wan:** Writing – review & editing, Conceptualization. **Jichun Ye:** Writing – review & editing, Conceptualization.

Declaration of competing interest

The authors declare that they have no known competing financial interests or personal relationships that could have appeared to influence the work reported in this paper.

Acknowledgement

We would like to thank Mr. Hongwei Kang and Junqian Zhizao Technology Co., Ltd as they provide the free-demo ozone gas equipment. This work was supported by the Ningbo “Innovation 2025” Major Project (2020Z098), the National Key R&D Program of China (Grant No. 2018YFB1500403), the National Natural Science Foundation of China (61974178, 61874177, 62004199), the Key Research and Development Program of Zhejiang Province (2021C01006), the Zhejiang Energy Group (Project No. znkj-2018-118), the Youth Innovation Promotion Association (2018333), the Zhejiang Provincial Natural Science Foundation (LY19F040002), Science and technology projects in Liaoning Province 2021 (2021JH1/10400104).

References

- [1] F. Feldmann, M. Bivour, C. Reichel, M. Hermle, S.W. Glunz, Passivated rear contacts for high-efficiency n-type Si solar cells providing high interface passivation quality and excellent transport characteristics, *Sol. Energy Mater. Sol. Cells* 120 (2014) 270–274.
- [2] Armin Richter, Benick Jan, Feldmann Frank, Fell Andreas, G.S.W. Hermle Martin, n-Type Si solar cells with passivating electron contact: identifying sources for efficiency limitations by wafer thickness and resistivity variation, *Sol. Energy Mater. Sol. Cells* 173 (2017) 96–105.
- [3] S. Schäfer, F. Haase, C. Hollemann, J. Hensen, J. Krügener, R. Brendel, R. Peibst, 26%-efficient and 2 cm narrow interdigitated back contact silicon solar cells with passivated slits on two edges, *Sol. Energy Mater. Sol. Cells* 200 (2019) 110021.
- [4] A. Richter, R. Müller, J. Benick, F. Feldmann, B. Steinhauser, C. Reichel, A. Fell, M. Bivour, M. Hermle, S.W. Glunz, Design rules for high-efficiency both-sides-contacted silicon solar cells with balanced charge carrier transport and recombination losses, *Nat. Energy* 6 (2021) 429–438.
- [5] J. Schmidt, R. Peibst, R. Brendel, Surface passivation of crystalline silicon solar cells: present and future, *Sol. Energy Mater. Sol. Cells* 187 (2018) 39–54.
- [6] Hongbo Tong, Industrialization Progression of 25.5% LONGi HPC Solar Cell. Xinyu Zhang (Jinko), Exploring Technological Progress and Mass Production of High-Efficiency N-type TOPCon Solar Cells, Seminar: large-scale Industrialization of TOPCon Technology, Beijing City, 2021, 09.17.
- [7] Y. Chen, D. Chen, C. Liu, W. Zigang, Y. Zou, Y. He, Y. Wang, L. Yuan, J. Gong, W. Lin, X. Zhang, Y. Yang, H. Shen, Z. Feng, P.P. Altermatt, P.J. Verlinden, Mass production of industrial tunnel oxide passivated contacts (i-TOPCon) silicon solar cells with average efficiency over 23% and modules over 345 W, *Prog. Photovoltaics* 27 (2019) 827–834.
- [8] D. Chen, Y. Chen, Z. Wang, J. Gong, C. Liu, Y. Zou, Y. He, Y. Wang, L. Yuan, W. Lin, R. Xia, L. Yin, X. Zhang, G. Xu, Y. Yang, H. Shen, Z. Feng, P.P. Altermatt, P. J. Verlinden, 24.58% total area efficiency of screen-printed, large area industrial silicon solar cells with the tunnel oxide passivated contacts (i-TOPCon) design, *Sol. Energy Mater. Sol. Cells* 206 (2020) 110258.
- [9] 2021 ITRPV, <https://itrpv.vdma.org/viewer/-/v2article/render/29775594>, 2021.
- [10] B. Kafle, B.S. Goraya, S. Mack, F. Feldmann, J. Rentsch, TOPCon – technology options for cost efficient industrial manufacturing, *Sol. Energy Mater. Sol. Cells* 227 (2021) 111100.
- [11] B. Steinhauser, J.I. Polzin, F. Feldmann, M. Hermle, S.W. Glunz, Excellent Surface Passivation Quality on Crystalline Silicon Using Industrial-Scale Direct-Plasma TOPCon Deposition Technology, *Solar RRL*, 2018, p. 1800068.
- [12] F. Frank, T. Fellmeth, B. Steinhauser, H. Nagel, D. Ourinson, M. Sebastian, E. Lohmuller, J. Polzin, J. Benick, A. Richter, A. Moldovan, M. Bivour, F. Clement, J. Rentsch, H. Martin, S.W. Glunz, Large area TOPCon cells realized by a PECVD process, in: 36th European PV Solar Energy Conference and Exhibition, France, Marseille, 2019.
- [13] C.K. Fink, K. Nakamura, S. Ichimura, S.J. Jenkins, Silicon oxidation by ozone, *J. Phys. Condens. Matter* 21 (2009) 183001.
- [14] A. Moldovan, F. Feldmann, G. Krugel, M. Zimmer, J. Rentsch, M. Hermle, A. Rothfölsch, K. Kai, C. Hagendorf, Simple cleaning and conditioning of silicon surfaces with UV/ozone sources, *Energy Proc.* 55 (2014) 834–844.
- [15] A. Moldovan, F. Feldmann, K. Kai, S. Richter, Tunnel oxide passivated carrier-selective contacts based on ultra-thin SiO₂ layers, *Sol. Energy Mater. Sol. Cells* 142 (2015) 123–127.
- [16] Y. Huang, M. Liao, Z. Wang, X. Guo, C. Jiang, Q. Yang, Z. Yuan, D. Huang, J. Yang, X. Zhang, Q. Wang, H. Jin, M. Al-Jassim, C. Shou, Y. Zeng, B. Yan, J. Ye, Ultrathin silicon oxide prepared by in-line plasma-assisted N₂O oxidation (PANO) and the application for n-type polysilicon passivated contact, *Sol. Energy Mater. Sol. Cells* 208 (2020) 110389.
- [17] D. Ma, W. Liu, M. Xiao, Z. Yang, Z. Liu, M. Q. H. Cheng, H. Xing, Z. Ding, B. Y. Wang, Y. Zeng, J. Ye, Highly Improved Passivation of PECVD P-type TOPCon by Suppressing Plasma-Oxidation Ion-Bombardment-Induced Damages, *Sol. Energy*, (submitted for publication).
- [18] Z. Yang, Z. Liu, M. Cui, J. Sheng, L. Chen, L. Lu, W. Guo, X. Yang, Y. Zhao, W. Yang, J.C. Greer, Y. Zeng, B. Yan, J. Ye, Charge-carrier dynamics for silicon oxide tunneling junctions mediated by local pinholes, *Cell Reports Physical Science* 2 (2021) 100667.
- [19] Q. Yang, M. Liao, Z. Wang, X. Guo, Z. Rui, D. Huang, J. Zheng, W. Guo, J. Sheng, P. Cheng, Y. Zeng, B. Yan, J. Ye, In-situ phosphorus-doped polysilicon prepared using rapid-thermal-process (RTP) annealing and its application for polysilicon passivated-contact solar cells, *Sol. Energy Mater. Sol. Cells* 210 (2020) 110518.
- [20] T. Gao, Q. Yang, X. Guo, Y. Huang, Z. Zhang, Z. Wang, M. Liao, C. Shou, Y. Zeng, B. Yan, G. Hou, X. Zhang, Y. Zhao, J. Ye, An industrially viable TOPCon structure with both ultra-thin SiO_x and n+-poly-Si processed by PECVD for p-type c-Si solar cells, *Sol. Energy Mater. Sol. Cells* 200 (2019) 109926.
- [21] X. Guo, M. Liao, Z. Rui, Q. Yang, Z. Wang, C. Shou, W. Ding, X. Luo, Y. Cao, J. Xu, L. Fu, Y. Zeng, B. Yan, J. Ye, Comparison of different types of interfacial oxides on hole-selective p+-poly-Si passivated contacts for high-efficiency c-Si solar cells, *Sol. Energy Mater. Sol. Cells* 210 (2020) 110487.
- [22] H. Tong, M. Liao, Z. Zhang, Y. Wan, D. Wang, C. Quan, L. Cai, P. Gao, W. Guo, H. Lin, C. Shou, Y. Zeng, B. Yan, J. Ye, A strong-oxidizing mixed acid derived high-quality silicon oxide tunneling layer for polysilicon passivated contact silicon solar cell, *Sol. Energy Mater. Sol. Cells* 188 (2018) 149–155.
- [23] R. Brendel, R. Peibst, Contact selectivity and efficiency in crystalline silicon photovoltaics, *IEEE J. Photovoltaics* 6 (2016) 1413–1420.

- [24] S.L. Peukert, R. Sivaramakrishnan, J.V. Michael, High temperature shock tube studies on the thermal decomposition of O₃ and the reaction of dimethyl carbonate with O-atoms, *J. Phys. Chem.* 117 (2013) 3729–3738.
- [25] K. Omiya, I.M. Rusinov, S. Suzuki, H. Itoh, Temperature dependence of ozone loss rate, *IEEJ Transactions on Fundamentals and Materials* 133 (2013) 465.
- [26] S.W. Benson, J. Arthur E. Axworthy, Mechanism of the gas phase, thermal decomposition of ozone, *J. Chem. Phys.* 26 (1957) 1718–1726. NUMBER 6.
- [27] C.K. Fink, K. Nakamura, S. Ichimura, S.J. Jenkins, Silicon oxidation by ozone, *J. Phys. Condens. Matter* 21 (2009) 183001.
- [28] Z. Liu, Z. Yang, W. Wang, Q. Yang, Q. Han, D. Ma, H. Cheng, Y. Lin, J. Zheng, W. Liu, M. Liao, H. Chen, Y. Wang, Y. Zeng, B. Yan, J. Ye, Numerical and experimental exploration for 26% rear-junction n-type silicon solar cells with front localized and rear full-area polysilicon passivated contact, *Sol. Energy* 221 (2021) 1–9.